JEE Journal of Ecological Engineering

Journal of Ecological Engineering 2022, 23(6), 58–66
https://doi.org/10.12911/22998993/147836
ISSN 2299–8993, License CC-BY 4.0

Received: 2022.03.14
Accepted: 2022.04.12
Published: 2022.04.20

Cerium-Promoted Nickel /Alumina Catalyst for Producer Gas Reforming and Tar Conversion

Salah H. Aljbour[1*], Katsuya Kawamoto[2]

[1] Chemical Engineering Department, Mutah University, 61710 Al-Karak, Jordan

[2] School of Environmental and Life Science, Okayama University, 3-1-1 Tsushima-naka, Okayama, 700-8530, Japan

* Corresponding author's e-mail: saljbour@mutah.edu.jo

ABSTRACT

The catalytic conversion of a model tar compound, namely: naphthalene contained in a simulated producer gas from wood gasification process was investigated. The sol-gel approach was used to create a mesoporous Ce-promoted Ni/alumina catalyst with high surface area. A surface area of 333 m^2/g was achieved by calcination of the mesoporous catalyst (17 wt% Ni and 2.8 wt% Ce) under air conditions at 1123 K. The catalysts were characterized using the N_2 adsorption-desorption, XRD, and SEM techniques, and their promotion effect on producer gas reforming and tar removal was studied under dry, steam, and partial oxidation conditions. The Ni-based catalysts effectively converted naphthalene and increased the proportion of H_2 and CO in the reformed gas. Incorporating Ce into the catalyst increased the proportion of H_2 and CO in the reformed gas, while lowering the amount of CH_4 and CO_2. In the absence of oxygen, catalytic reforming of the producer gas resulted in 79.6% naphthalene conversion, whereas catalytic partial oxidation conditions resulted in 99.1% naphthalene conversion.

Keywords: cerium; nickel; tar; naphthalene; catalyst; gasification; reforming.

INTRODUCTION

Biomass gasification has been identified as a promising strategy for producing renewable energy. It is regarded as one of the most effective technologies for replacing fossil fuels [Situmorang et al., 2020]. Gasification of biomass is a thermochemical process that converts biomass into synthesis gas. This can be accomplished by using gasifying agents such as air, oxygen and/or steam [Moilanen et al., 2009]. The conversion of biomass fuel gas to syngas is a critical step in the exploitation of biomass since syngas serves as a building block for various chemicals, such as methanol, dimethyl ether, and higher hydrocarbons via the Fischer-Tropsch process [Wang et al., 2008].

One of the promising routes for hydrogen production is biomass gasification; such a fuel is regarded as a clean energy carrier [Cao et al., 2020]. In addition, gasification offers the intrinsic flexibility of being able to process a variety of feedstocks from industry and agriculture [Yassin et al., 2009], contributing to a cleaner environment.

Nevertheless, the production of tar and particulates is a major issue associated with biomass gasification. The presence of such contaminants in the producer gas causes the technical issues with downstream process equipment such as gas engines and turbines [Aljbour and Kawamoto, 2013a; Aljbour and Kawamoto, 2013b]. Engine or turbine applications necessitate the use of a low-tar producer gas.

One problem of typical gasification systems is the high temperature operation required to reduce the activation energy of the complicated gasification and reforming reactions. Certainly, the application of catalysts can lower the operating temperature. Extensive research has been published on the design and use of catalysts for biomass-derived gas reforming and tar destruction. Catalyst use downstream of the gasification zone may aid in gas reforming and tar destruction

[Yu et al., 2021; Narnaware and Panwar, 2021; Galadima et al., 2022]. Nickel-containing catalysts have piqued the interest of numerous researchers due to their inexpensive cost and wide range of industrial uses in the petrochemical industry [Wu et al., 2021].

At high reaction temperatures, Ni-based catalysts are effective for cleavage of the C-H, C-C, and O-H bonds of biomass-derived oxygenated compounds to form the producer gas [Micheli et al., 2017]. Supported nickel catalysts, in particular, are cost-effective and efficient for producing H_2 and CH_4 from various biomass sources. As they catalyze the methane steam/dry reforming and the water-gas-shift processes, supported nickel catalysts give improved gasification efficiency and hydrogen yields. Because of their fluidizability, large surface areas, and ease of forming into pellets, alumina is the most often utilized mesoporous support for Ni-based catalysts [Enríquez et al., 2022]. Unfortunately, sintering and/or coke deposition frequently deactivate Ni catalysts [Bulushev and Ross, 2011]. Incorporating certain promoters such as oxides of rare earth metals into nickel catalysts improved the catalyst resistance to coking and sintering. Cheng et al. [Cheng et al., 1996] have reported that promoters such as lanthanide oxides could exert a promotion effect on the initial activity of CO_2 reforming of methane over Ni/Al_2O_3 catalysts. Borowiecki et al. [Borowiecki et al., 1998] have shown that the addition of small amount of cerium into a Ni catalyst has a favorable influence on the nickel dispersion and its resistance for sintering. Wang and Lu [Wang and Lu, 2000] have noticed higher catalytic stability and suppression of carbon deposition during CO_2 reforming of methane when using La_2O_3 or CeO_2-promoted Ni/γ-Al_2O_3 catalysts. Natesakhawat et al. [Natesakhawat et al., 2005] have reported an improvement in both catalytic stability and activity of ytterbium- and cerium-promoted Ni-based catalysts during steam reforming of propane.

The present study investigated the use of cerium-promoted nickel/alumina catalyst for simultaneous producer gas reforming and tar removal. The prepared catalysts were characterized and their promotion effect on producer gas reforming as well as tar removal was examined under dry reforming, steam reforming and partial oxidation conditions.

EXPERIMENTAL

Catalyst preparation and characterization

The catalysts were prepared by sol-gel procedures. $Ni(NO_3)_2.6H_2O$ and $Ce(NO_3)_2.6H_2O$ were used for the nickel and cerium precursors. Aluminum tri-sec butoxide (ATB) was used as an aluminum precursor. The preparation procedure began by gradual addition of ATB in ethanol while being stirred vigorously. The resulting ATB-ethanol mixture was heated to a temperature of 353 K. Pre-dissolved nickel and cerium precursor in a required amount of DI water and ethanol were added to the ATB-ethanol mixture under vigorous stirring at a flow rate of 0.5 ml/min by means of a syringe pump. The amount of water used was equivalent to twice the moles of ATB being used and one additional mol of water per liter of ethanol being used. The total amount of ethanol used was fixed at 400 ml. After the addition of the nickel and cerium solution, the resulting gel was stirred for another 2 hr at 358 K to evaporate the remaining alcohol then dried overnight in an oven at 353 K. Calcination of the dried catalysts were carried out under air conditions at 1123 K for 5 hours. Reduction of catalysts was done at elevated temperature with an H_2 stream diluted with N_2 (200 ml/min, 10 vol% H_2) for 3 hrs.

The BET surface area of calcinated catalysts were measured by N_2 adsorption-desorption at 77 K (Quadrasorb USA). Prior to measurements, the samples were degassed under vacuum at 573 K for 8 hrs.

The X-ray diffraction (XRD) patterns were obtained by using a powder X-ray diffractometer (Bruker AXS D8 Advance) with graphite monochromatized Cu-Kα radiation at 40 kV and 40 mA.

A scanning electron microscope (SEM) was used to examine the morphology of the catalysts (OXFORD instruments).

Experimental setup

Figure 1 shows a schematic drawing of the experimental setup. Catalytic reforming of the producer gas and tar decomposition experiments were carried out in a tubular stainless steel reactor (12 mm ID). A split-type tube furnace was used to heat the reactor from the outside. The catalyst was loaded into the middle of reactor at wool-made bed. A PID controller was used to control the temperature of the catalyst bed.

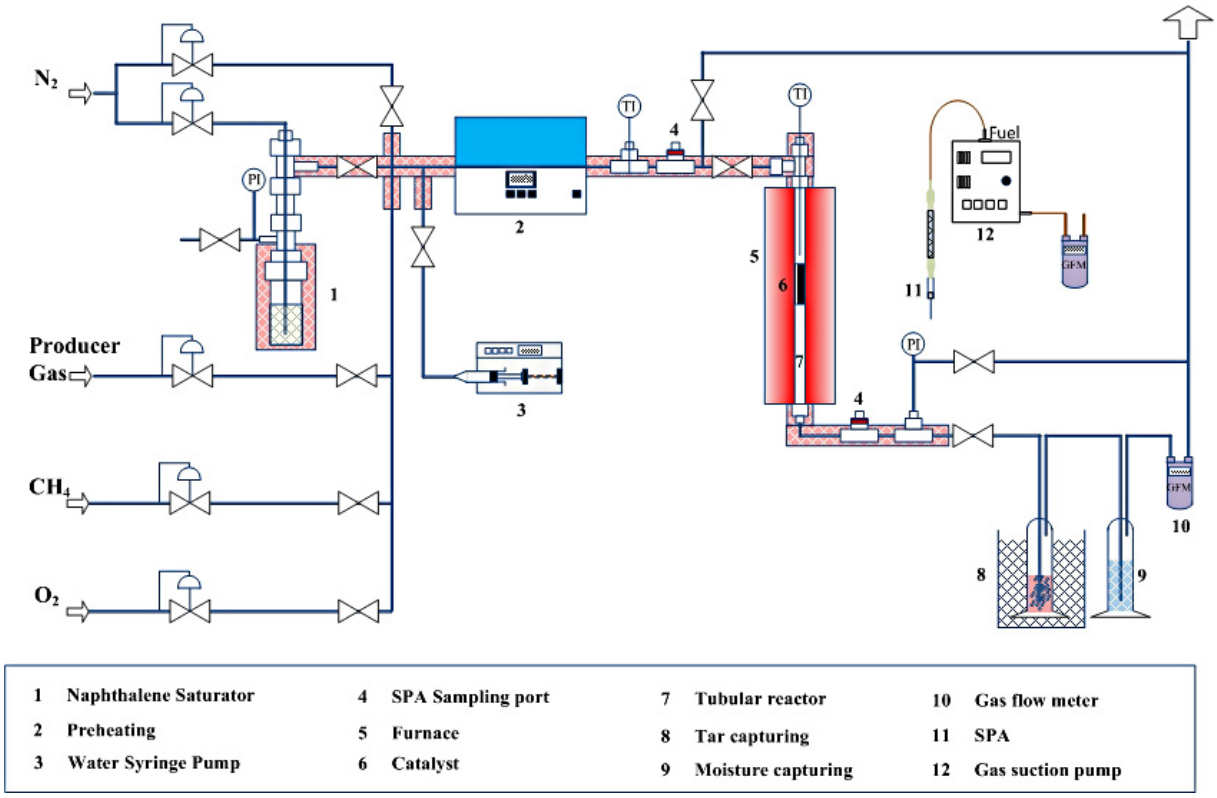

Figure 1. Experimental setup

A simulated producer gas was used in the experimentation. The producer gas comprised a mixture of gases, namely: H_2, CO, CO_2, CH_4, O_2, and N_2. Naphthalene was chosen as a model tar compound because it is one of the most stable tars and hence one of the most difficult to remove. A typical naphthalene concentration in a producer gas from a wood gasification process was employed in this investigation, with an input naphthalene concentration of 1 g/Nm^3. To create naphthalene vapor, a naphthalene saturator heated by a mantle heater was employed.

A nitrogen stream was used to sweep the naphthalene vapor, which was then mixed with the simulated producer gas stream. To obtain the appropriate producer gas and tar composition, the resultant gas stream was diluted with another nitrogen stream. A syringe pump was used to add water to the producer gas stream. The resultant gaseous stream was preheated to 653 K to avoid condensation in the tubes.

Prior to analysis, the tar and moisture are removed from the reformed gas stream. TEDLAR sampling bags are used to collect samples of the reformed gas from the downstream line on a regular basis. The tar-free gas is analyzed by using two micro-GC 3000 (Agilent Technologies). The gas instrumental analysis system is described in detail elsewhere [Aljbour and Kawamoto, 2013a].

The Solid Phase Adsorption (SPA) technique is used to sample naphthalene [Brage et al., 1997]. SPA columns having a size of 3 ml were used (SampliQ Amino, Agilent Technologies). Using a gas sampling pump (GSP-250FT, GASTEC Co., Yamato), 100 ml of the gas was collected from the sampling port at a rate of 50 ml/min. Elution with 2 ml dichloroethane under positive pressure from a syringe recovered the trapped tar from the SPA column. Quantitative analysis on the collected solution was carried out via a GC/MS (Shimadzu Co.).

RESULTS AND DISCUSSION

Catalyst characterization

The catalysts with different Ni and Ce loadings were prepared by sol-gel techniques. The Ni and Ce loadings in the catalysts are reported based on the initial amounts of Ni and Ce utilized in the preparation of the catalyst. The nitrogen adsorption–desorption isotherms of the produced catalysts are shown in Figure 2.

Although Ni and Ce were loaded on the support, all of the catalysts displayed type IV hysteresis loop isotherms, showing that the mesoporous texture could be preserved to a great extent.

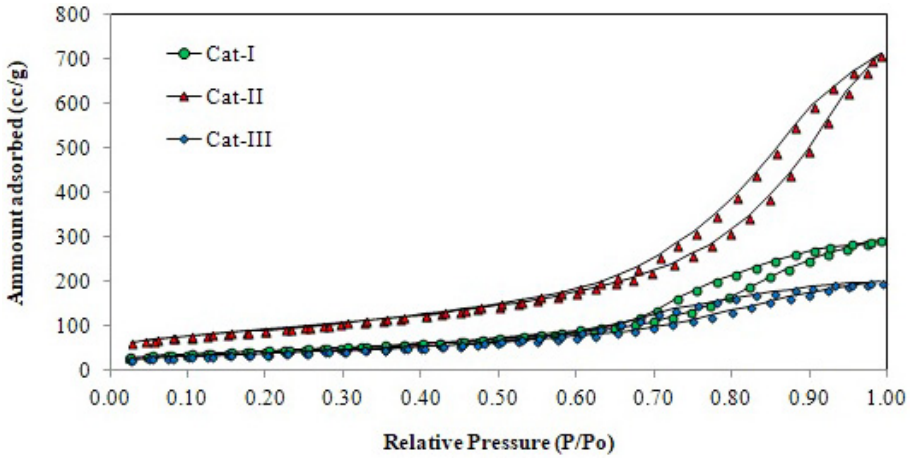

Figure 2. Nitrogen adsorption and desorption isotherms of Ni-Ce/Alumina catalysts

Table 1. The physical properties of catalysts

Catalyst ID	Ni wt%	Ce wt%	BET (m^2/g)	Pore size ($A°$)
Cat-I	20	0	159	75
Cat-II	17	2.8	333	66
Cat-III	18	6	141	44

The BET surface area and the average pore diameter of catalysts are shown in Table 1.

The inclusion of Ni and Ce obviously increased the surface area of catalyst. This might be owing to the adoption of the sol-gel process in catalyst synthesis, which results in a uniform distribution of metal in the support matrix. The active metal precursors are also likely to have induced surface roughening on the alumina support [Guggilla et al., 2010]. However, when the Ce loading was excessively increased, the BET surface area and pore volume both decreased. This might be ascribed to an interaction between the active phase precursor and the surface groups of the support. A surface response like this might have reduced the accessible surface area of the substrate, most likely by closing the pores.

In Figure 3, the XRD patterns of the catalysts are compared. The XRD patterns of both catalysts were identical. $NiAl_2O_4$ and NiO are potential crystalline phases in both catalysts. Cerium-related crystalline phases could not be confirmed based on the XRD pattern of Cat-II. It is possible that the Ce is well-distributed or exists as a

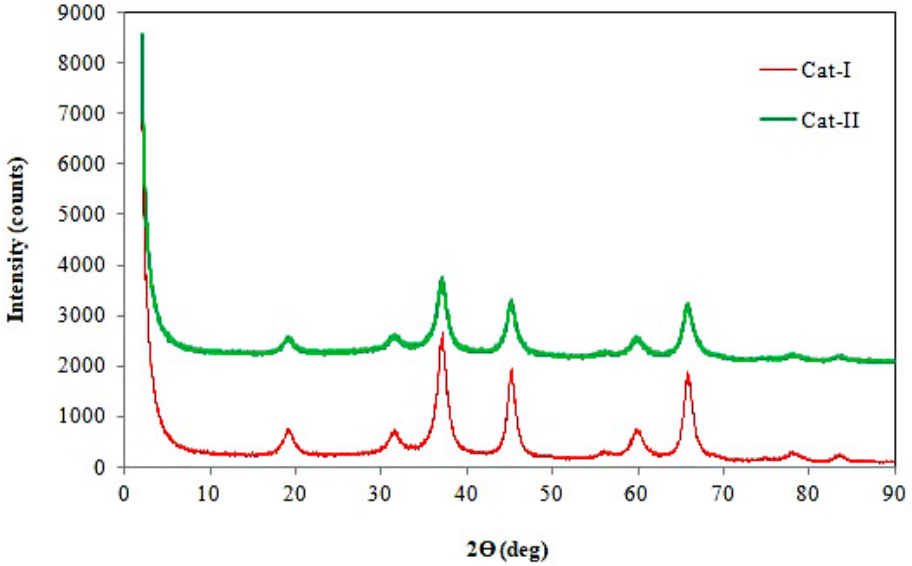

Figure 3. XRD patterns of the catalysts

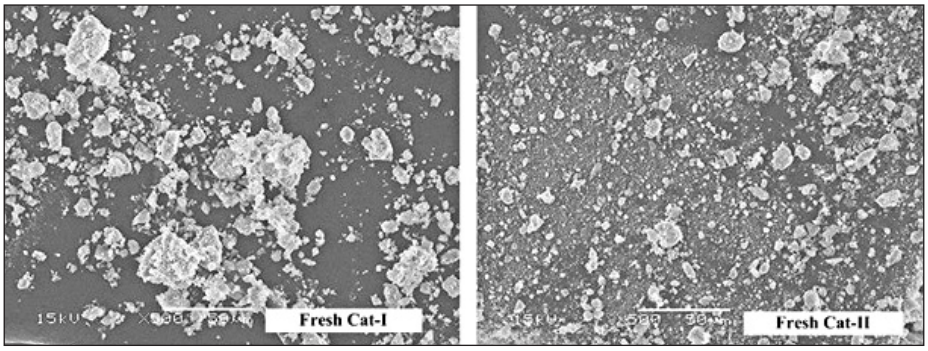

Figure 4. SEM images of the fresh catalysts

two-dimensional overplayed on the Ni aluminum oxide layer that is undetected by XRD [Natesakhawat et al., 2005].

SEM was used to examine the surface morphologies of the produced catalysts. The images of Cat-I and Cat-II were enlarged 500 times each. The bright areas of the SEM images, as seen in Figure 4, represented the metal surfaces of the catalysts.

The catalysts were made up of grains of varying shapes and sizes. However, in Figure 4, the grain size was lower in the SEM images of Cat-II compared to Cat-I. In the presence of Ce promoter, it is suggested that nickel particles combined with the promoter be spread finely over the support surface without agglomeration.

Catalytic reforming of the producer gas

The performance of the prepared catalysts has been examined under producer gas steam reforming conditions. Table 2 shows the reformed producer gas composition and naphthalene conversion when using the three catalysts.

The results indicate clearly the promotion effect of the catalysts in producer gas reforming and naphthalene conversion. The Ni-based catalysts achieved almost complete conversion of naphthalene and increased the proportion of H_2 and CO in the reformed gas.

Incorporating Ce within the catalyst enhanced the proportion of H_2 and CO and reduced the content of CH_4 and CO_2 in the reformed gas as a result of CO_2 reforming:

$$CH_4 + CO_2 \longrightarrow 2CO + 2H_2 \quad (1)$$

The methane gas could be also consumed via steam reforming:

$$CH_4 + H_2O \longrightarrow CO + 3H_2 \quad (2)$$

The methane gas could be also consumed via partial oxidation:

$$CH_4 + \tfrac{1}{2}O_2 \longrightarrow 2CO + 2H_2 \quad (3)$$

The actively and stability of the prepared sol-gel catalysts were examined by monitoring the CH_4 conversion as a function of time (Figure 5).

An inspection of Figure 5 shows that the sol-gel prepared catalysts showed high activity toward CH_4 conversion. The maximum CH_4 conversions were 89, 98 and 99% when using Cat-I, Cat-II and Cat-III respectively. However, the catalysts exhibited a decline in activity with time on stream. Cat-I rapidly indicated a decline in the catalytic activity, while Cat-II and Cat-II could

Table 2. Producer gas composition and naphthalene conversion under catalytic steam reforming condition (steam-to-gas volume ratio = 0.06, temperature = 750 °C)

Compund/Element	Feed	Cat-I	Cat-II	Cat-III
H_2 (vol %)	15.9	16	21	17
CO (vol %)	9.5	14.6	12.2	11.8
CO_2 (vol %)	4.8	3.2	3.8	3.7
CH_4 (vol %)	1.3	0.3	0.05	0.17
O_2 (vol %)	0.6	0.3	0.13	0.1
N_2 (vol %)	Balance			
H_2/CO (-)	-	1.1	1.7	1.4
Naphthalene conversion (%)	-	99.1	99.8	99.3

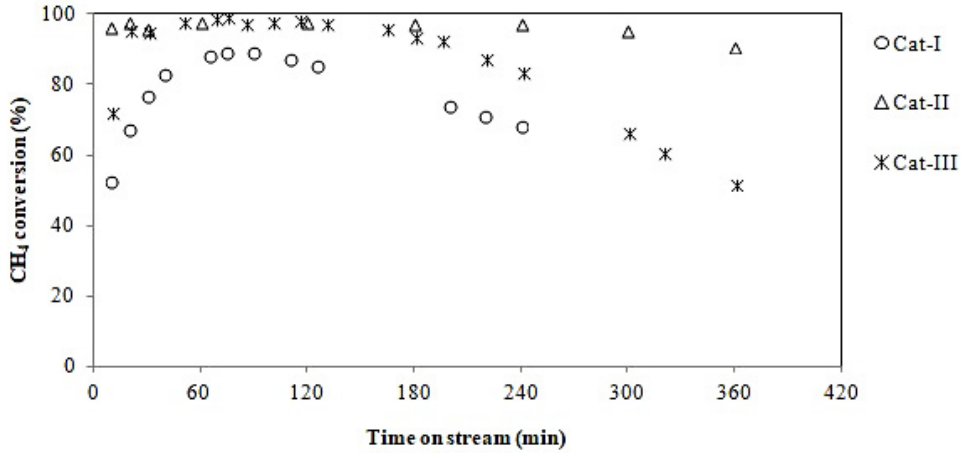

Figure 5. Profile of CH_4 conversion under catalytic steam reforming conditions (steam-to-gas volume ratio = 0.06, temperature = 750 °C)

maintain longer catalytic activity as a result of the presence of Ce within the matrix of the catalyst.

Figure 6 shows the CH_4 conversion as a function of time when using fresh and regenerated Cat-I under steam reforming condition.

Catalyst regeneration was conducted by burning off the catalyst at a temperature of 750°C under oxygen flow. The results shown in Figure 6 indicate that burning off the catalyst could maintain the initial activity of the catalyst and confirm that catalyst deactivation was caused by coke formation. Coke is typically formed during the cracking of methane, the Boudouard reaction, and the reduction of CO to carbon, as follows [Arman et al., 2020]:

$$CH_4 \longrightarrow C + 2H_2 \quad (4)$$

$$2CO \longrightarrow C + CO_2 \quad (5)$$

$$CO + 3H_2 \longrightarrow C + H_2O \quad (6)$$

As indicated by Eq. (7) and Eq. (8), naphthalene may be reformed on a catalyst surface with either steam or carbon dioxide, or both, yielding more H_2 and CO [Buchireddy et al., 2010].

$$C_{10}H_8 + 10H_2O \longrightarrow 10CO + 14H_2 \quad (7)$$

$$C_{10}H_8 + 10CO_2 \longrightarrow 20CO + 4H_2 \quad (8)$$

In addition, the naphthalene conversion could be further enhanced by partial oxidation. Table 3 compares the producer gas reforming in the absence and presence of oxygen in the producer gas.

Catalytic reforming of the producer gas in the absence of oxygen has promoted 79.6% naphthalene conversion. The presence of oxygen is essential for complete naphthalene conversion via partial oxidation. Wang et al. [Wang et al., 2008] investigated the partial oxidation reforming of biomass fuel gas using naphthalene as a model tar

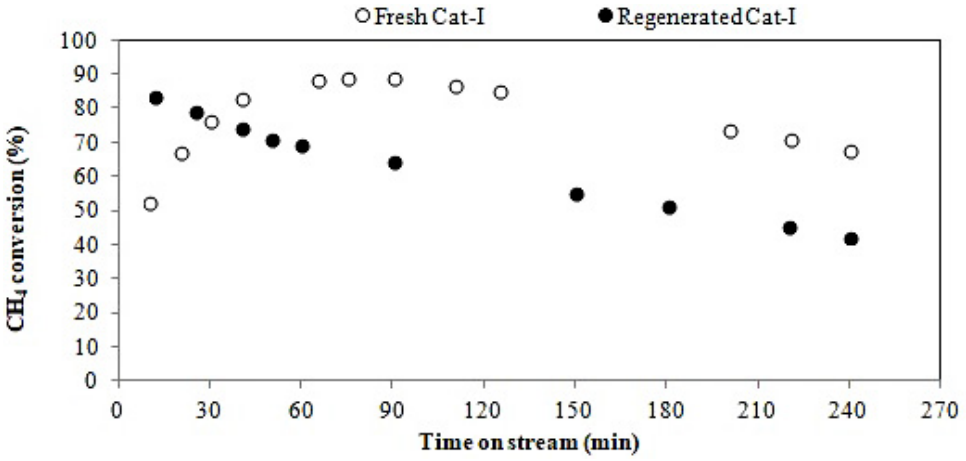

Figure 6. CH_4 conversion as a function of time when using fresh and regenerated Cat-I under steam reforming condition (steam-to-gas volume ratio = 0.06, temperature = 750 °C)

Table 3. Producer gas composition and naphthalene conversion under catalytic reforming condition (steam-to-gas volume ratio = 0.06, temperature = 750 °C, Cat-II)

Compound/Element	Feed 1	Reformed gas 1	Feed 2	Reformed gas 2
H_2 (vol %)	15.9	21	15.9	21
CO (vol %)	9.5	12.2	9.5	14
CO_2 (vol %)	4.8	3.8	4.8	1
CH_4 (vol %)	1.3	0.05	1.3	0.16
O_2 (vol %)	0.6	0.13	0	0
N_2 (vol %)	Balance			
Naphthalene conversion (%)	-	99.1	-	79.6

compound over a nickel-based monolithic catalyst. According to the researchers, the addition of O_2 can effectively prevent the formation of coke and enhance tar conversion.

Figure 7 shows the maximum CH_4 conversion as a function of the initial CH_4 concentration in the producer gas.

The catalytic conversion of methane is affected by the initial concentration of CH_4 in the producer gas. High conversion of CH_4 could be achieved under smaller initial concentrations.

SEM was again used to examine the surface morphologies of the used catalysts. The images of spent Cat-I and Cat-II were compared under 500 image magnifications (Figure 8).

The catalysts were made up of various shaped and sized grains. When comparing spent Cat-II to fresh Cat-II, the grain size was higher in the SEM image of spent Cat-II. Catalyst grains agglomerated as a result of high temperature operation and longer time on stream operation.

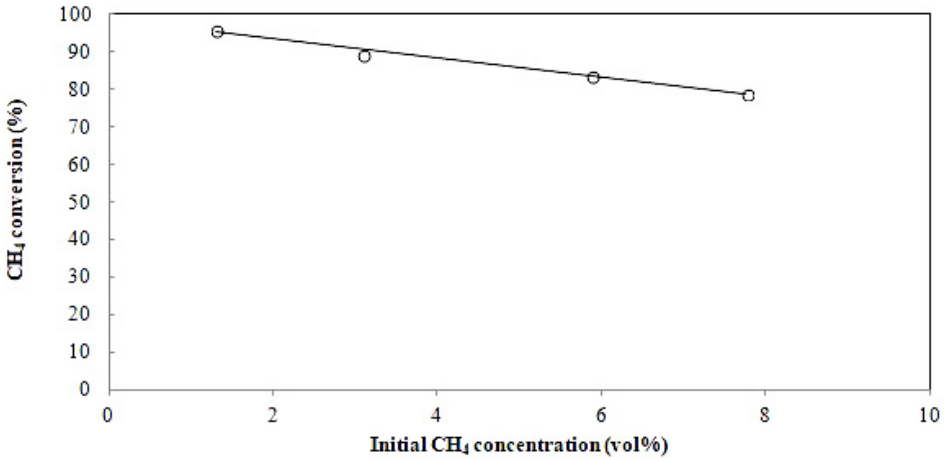

Figure 7. Maximum CH_4 conversion as a function of the initial CH_4 concentration in the producer gas (dry reforming, temperature = 750 °C, Cat-II)

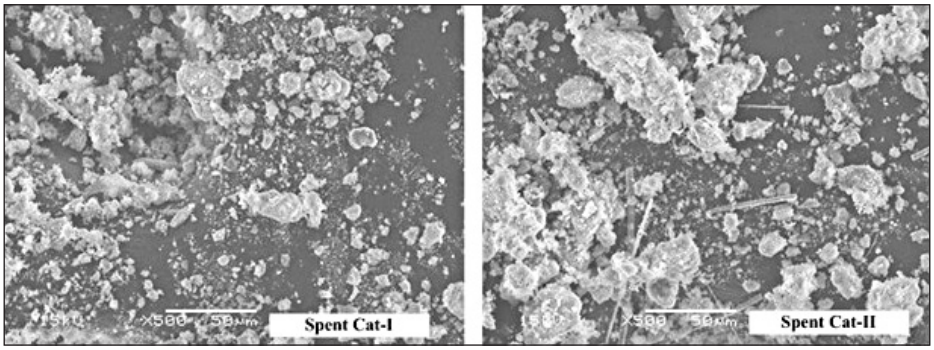

Figure 8. SEM images of the spent catalysts

CONCLUSIONS

A mesoporous Ce-promoted Ni/alumina catalyst with a large surface area was successfully prepared by using the sol-gel method. The mesoporous catalyst containing 17 wt% Ni and 2.8 wt% Ce, and obtained through calcination at air conditions at 1123 K had a surface area of 333 m^2/g. The produced catalysts were characterized, and their promotion effect on producer gas reforming and tar removal was investigated under dry, steam, and partial oxidation conditions.

The Ni-based catalysts converted naphthalene almost completely and enhanced the amount of H_2 and CO in the reformed gas. Incorporating Ce into the catalyst increased the fraction of H_2 and CO while decreasing the quantity of CH_4 and CO_2 in the reformed gas.

Catalytic reforming of the producer gas in the absence of oxygen resulted in 79.6% naphthalene conversion, whereas the catalytic partial oxidation conditions resulted in 99.1% naphthalene conversion.

REFERENCES

1. Aljbour S.H., Kawamoto K. 2013a. Bench-scale gasification of cedar wood–Part I: Effect of operational conditions on product gas characteristics. Chemosphere, 90, 1495–1500.
2. Aljbour S.H., Kawamoto K. 2013b. Bench-scale gasification of cedar wood–Part II: Effect of operational conditions on contaminant release. Chemosphere, 90, 1501–1507.
3. Arman A., Hagos F., Abdullah A., Mamat R., Aziz A., Cheng C. Syngas production through steam and CO2 reforming of methane over Ni-based catalyst - A Review. IOP Conference Series: Materials Science and Engineering, 2020. IOP Publishing, 042032.
4. Borowiecki T., Gołebiowski A., Ryczkowski J., Stasinska B. 1998. The influence of promoters on the coking rate of nickel catalysts in the steam reforming of hydrocarbons. Studies in Surface Science and Catalysis, 711–716.
5. Brage C., Yu Q., Chen G., Sjöström K. 1997. Use of amino phase adsorbent for biomass tar sampling and separation, 76, 137–142.
6. Buchireddy P.R., Bricka R.M., Rodriguez J., Holmes W. 2010. Biomass gasification: catalytic removal of tars over zeolites and nickel supported zeolites. Energy and Fuels, 24, 2707–2715.
7. Bulushev D.A., Ross J.R. 2011. Catalysis for conversion of biomass to fuels via pyrolysis and gasification: a review. Catalysis Today, 171, 1–13.
8. Cao L., Iris K., Xiong X., Tsang D.C., Zhang S., Clark J.H., Hu C., Ng Y.H., Shang J., Ok Y.S. 2020. Biorenewable hydrogen production through biomass gasification: A review and future prospects. Environmental Research, 186, 109547, https://doi.org/10.1016/j.envres.2020.109547
9. Cheng Z., Wu Q., Li J., Zhu Q. 1996. Effects of promoters and preparation procedures on reforming of methane with carbon dioxide over Ni/Al2O3 catalyst. Catalysis Today, 30, 147–155.
10. Enríquez A.S., Castañeda D.G.G., Hernández A.R.C., Reyes I.C., Rosales B.S. 2022. Hydrogen production via surrogate biomass gasification using 5% Ni and low loading of lanthanum co-impregnated on fluidizable γ-alumina catalysts. International Journal of Chemical Reactor Engineering, 22, 17–33.
11. Galadima A., Masudi A., Muraza O. 2022. Catalyst development for tar reduction in biomass gasification: Recent progress and the way forward. Journal of Environmental Management, 305, 114274, https://doi.org/10.1016/j.jenvman.2021.114274
12. Guggilla V.S., Akyurtlu J., Akyurtlu A., Blankson I. 2010. Steam reforming of n-dodecane over Ru− Ni-based catalysts. Industrial and Engineering Chemistry Research, 49, 8164–8173.
13. Micheli F., Sciarra M., Courson C., Gallucci K. 2017. Catalytic steam methane reforming enhanced by CO2 capture on CaO based bi-functional compounds. Journal of Energy Chemistry, 26, 1014–1025.
14. Moilanen A., Nasrullah M., Kurkela E. 2009. The effect of biomass feedstock type and process parameters on achieving the total carbon conversion in the large scale fluidized bed gasification of biomass. Environmental Progress and Sustainable Energy: An Official Publication of the American Institute of Chemical Engineers, 28, 355–359.
15. Narnaware S.L., Panwar N. 2021. Catalysts and their role in biomass gasification and tar abetment: a review. Biomass Conversion and Biorefinery, 1–31, https://doi.org/10.1007/s13399-021-01981-1
16. Natesakhawat S., Oktar O., Ozkan U.S. 2005. Effect of lanthanide promotion on catalytic performance of sol–gel Ni/Al2O3 catalysts in steam reforming of propane. Journal of Molecular Catalysis A: Chemical, 241, 133–146.
17. Situmorang Y.A., Zhao Z., Yoshida A., Abudula A., Guan G. 2020. Small-scale biomass gasification systems for power generation (< 200 kW class): A review. Renewable and Sustainable Energy Reviews, 117, 109486, https://doi.org/10.1016/j.rser.2019.109486
18. Wang C.G., Wang T.J., Ma L.L., Gao Y., Wu C.Z. 2008. Partial oxidation reforming of biomass fuel gas over nickel-based monolithic catalyst with naphthalene as model compound. Korean Journal of Chemical Engineering, 25, 738–743.

19. Wang S., Lu M.G. 2000. Reaction kinetics and deactivation of Ni-based catalysts in CO_2 reforming of methane. Reaction engineering for pollution prevention. Edited by Martin A. Abraham and Robert P. Hesketh. New York: Elsevier, 75–84.
20. Wu L., Xie X., Ren H., Gao X. 2021. A short review on nickel-based catalysts in dry reforming of methane: Influences of oxygen defects on anti-coking property. Materials Today: Proceedings, 42, 153–160.
21. Yassin L., Lettieri P., Simons S.J., Germanà A. 2009. Techno-economic performance of energy-from-waste fluidized bed combustion and gasification processes in the UK context. Chemical Engineering Journal, 146, 315–327.
22. Yu J., Guo Q., Gong Y., Ding L., Wang J., Yu G. 2021. A review of the effects of alkali and alkaline earth metal species on biomass gasification. Fuel Processing Technology, 214, 106723, https://doi.org/10.1016/j.fuproc.2021.106723